Academic Journal of Research and Scientific Publishing | Vol 4 | Issue 48
Publication Date: 05-04-2023 ISSN: 2706-6495

Design and Simulation of Transceiver Antennas in FSO Technology within the 5G Networks

Mansour H. Almalki[1*], Adnan Affandi[1], and Avez Syed[1]

Electrical and Computer Engineering Department, Faculty of Engineering, King Abdulaziz University, P.O. Box 80204, Jeddah 21589, Saudi Arabia [1]

[*]Email: ms.515@hotmail.com

Abstract:

There is an urgent need for high-capacity connection with high data transfer rate in densely populated areas due to the rapid growth of mobile communication technologies and the explosion of data traffic. Multi beam antennas have generated a lot of research interest and have been extensively explored for base station applications due to their ability to boost communication capacity and sustain a high data transfer rate. Multi-beam antennas based on Butler matrices (MABBMs) are also appropriate for base station applications because to their advantages of high gain, simple design, and low profile. This paper's goal is to give a summary of the current MABBMs. The presentation of MABBMs includes its specifications, operating principles, design methodology, and implementation. In the final section, the difficulty of MABBMs for 3G/LTE/5G/B5G base station applications is discussed.

The paper is divided into six sections, in the first section an introduction, in the second section base station application standards are presented, the design strategy and operating principles of MABBMs in the third section, and the latest developments in MABBM research for mobile communication systems are addressed in the fourth section, and challenges are presented in fifth Section, and conclusions are presented in the sixth Section.

Keywords: Transceiver antennas, Free-space optical, Fifth generation networks.

1. Introduction

With the rapid advancement of mobile communication technology and the expansion of data traffic, high-capacity connectivity is urgently required in densely populated places. Two primary conventional strategies are typically used to boost the channel capacity for mobile communications. One is to use wideband or multiband antennas to increase the frequency bandwidth. (LI M et al., 2018), (HUANG H et al., 2020), and the other is to divide a sector into multiple ones by using multibeam antennas (SUDHAKAR et al., 1995), (WINCZA et al., 2017). Additionally, each of the two techniques—wideband/multiband and multi beam operation—can be employed at the same time to further increase the communication capacity. A wideband or dual-band multi beam antenna, for instance, can be used in place of a standard sector base station antenna to increase capacity. Multi-beam antenna technology, one of the foundational elements of 5G communications, is also capable of providing high data transmission rates, improved signal-to-interference-plus-noise ratios, increased spectral and energetic efficiency, and flexible beam shaping. It is widely used for 3G/LTE/5G mobile communication and is a system. the new system for B5G mobile communication. (HONG et al., 2017)

There are various common techniques that have been used to implement the design of a multi beam antenna. An aerial reflector is one strategy. Placing numerous feeds in various positions in front of a reflector aerial will make it simple to obtain multiple beams radiating at various angles. (SUDHAKAR et al., 1995), (CHOU et al., 2018). Using a lens aerial is a different method. (MANOOCHEHRI et al., 2018), (MEI Z L et al., 2012). When a lens is activated by several feeds at various points, the focusing or reflecting function of the lens can vary the direction in which the electromagnetic wave propagates, producing numerous radiation beams. (HUANG M et al., 2014), (JIANG Z H et al., 2012)

Reflector-based and lens-based multi beam antennas, while typically adequate for millimeter wave frequencies, suffer from huge dimensions and are therefore unsuitable for sub-6 GHz base station applications.

Because to the benefits of high gain, low profile, and simple structure, multi beam antennas fed by Butler matrices (WU Q et al., 2018), (HONG et al., 2017), they are expected to be an effective

solution of multi-beam antenna for 3G/LTE/ 5G/B5G mobile communication systems. In this paper, the multi-beam antennas based on Butler matrix (MABBM) technologies are reviewed.

The structure of this article is as follows.

The standards for base station applications are covered in part 2. The design strategy and operating principles of MABBMs are presented in part 3. The most recent developments in MABBM research for mobile communication systems are covered in part 4. Challenges are presented in Section 5, and conclusions are presented in Part 6.

2. Specifications for Base-Station

Applications A few crucial MABBM parameters should be necessary for real-world base station applications.

The first is that in order to provide good coverage, multiple beams must maintain a consistent 10 dB beam width of approximately 120° in the horizontal plane.

The second requirement is that for effective communication, the cross level between adjacent beams must be around 10 dB, as seen in Fig. 1.

Signals from two sectors will overlap if it is set too high, resulting in continuous handoff.

On the other hand, if the cross level is too low, good coverage is not necessarily ensured.

The third requirement is that each beam's side and grating lobes must be suppressed at a low level to minimize signal interference with nearby beams.

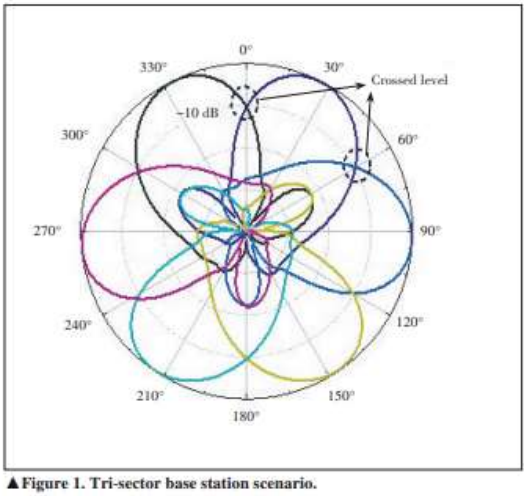

▲Figure 1. Tri-sector base station scenario.

Because of this, base stations in highly populated locations urgently need MABBMs with such performances over a large frequency band or several frequencies.

A. FSO Transceiver Design

Fig.(a) shows the optical route and system design of our suggested FSO transceiver. In order to effectively regulate the received light deflection angle and fibre coupling, five VCM actuators were built to control the 3-axis position of the lenses located on the receiving and transmitting optical path. Our miniature VCM actuator and lens measure 12 mm * 12 mm * 5 mm and 8 mm, respectively, as illustrated in Fig. (b).

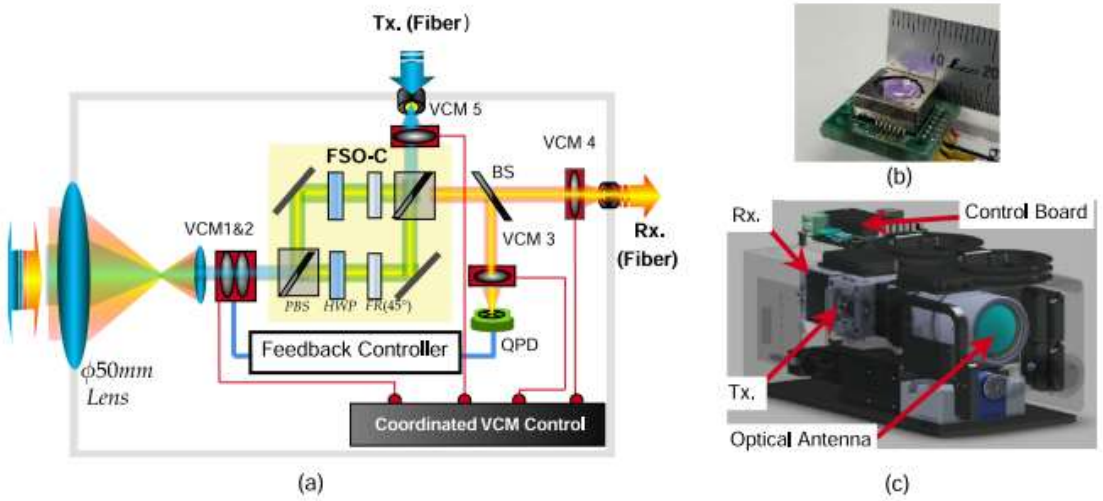

We created a 3-port, polarization-independent FSO-C for the first time, with properties resembling those of a fiber-based optical circulator, to enable fiber-to-fiber and full-duplex transmission. It is made up of a polarizing beam splitter (PBS), a prism mirror, a half-wave plate (HWP), and a 45° Faraday rotator (FR). In this circulator, the insertion loss is less than 0.5 dB, and the isolation between the three ports is greater than 25 dB.

Contrary to the fiber-based optical calculator, which can be installed at the FSO transceiver's receiving port, the FSO-C can enable effective and independent control of the transmitted and received beams, much like the binocular FSO transceiver, which results in a straightforward and adaptable optical path design.

In fact, the FSO-C, especially for narrow beam FSO links and moving platforms, will not only permit full-duplex transmission but will also completely eliminate the effect of the optical aerial roll. The incoming laser beam emitted from the SMF is aligned and extended to the φ2 mm beam by altering the 3D location of the VCM5 lens. Before being transmitted to the air, the collimated beam proceeds via the FSO-C and a 1:7.5 beam expansion process to reach a diameter of about φ15 mm..

A 50 mm lens is used to accept the beam at the receiving end, which is then aligned using VCM1&2 and fed via the FSO-C. The beam is then seamlessly coupled to the fiber core using both the fine tracking module based on VCM1&2 and the fiber coupling module based on VCM4. We used a 10:90 beam splitter and a QPD as a tracking sensor to run the fine tracking module.

In actuality, the QPD sensor performs better than image sensors in terms of response time and beam position accuracy (I. A. Ivan et al., 2012). The lens location (x, y) was initially adjusted so that the laser beam spot is centered at the QPD aperture, and its z-value is utilized to control the beam spot size. We then added another VCM actuator (i.e., VCM3) to concentrate the beam to the QPD sensor. The proportional-integral-derivative (PID) controller used the predicted slanted angle of the received wave front to order the VCMs 1 and 2 in a way that minimized the deflection angle.

We used a commercial VCM actuator in this terminal that was created expressly for use with smartphone cameras, where the control bandwidth was up to 100 Hz. Due to I the closed-loop servo bandwidth, (ii) the used off-the-shelf VCM technology bandwidth (that is developed for smartphone camera), and (iii) the adjustable lens weight, the control bandwidth in our system was restricted to up to 100 Hz. To maximize the bandwidth, the PID controller's parameters were carefully modified in both the x and y axes.

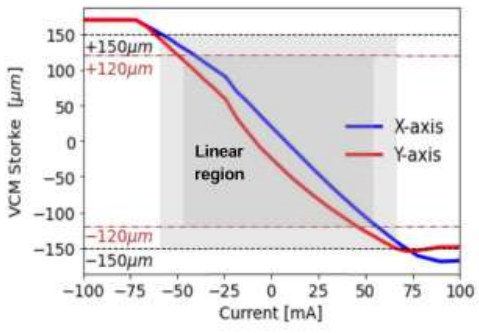

Fig E. VCM actuator stroke vs. applied current.

The response of our VCM stroke (m) to the applied current is shown in Fig. E. (mA). According to the picture, the VCM will travel linearly from 120 m to +120 m, with a full stroke of 240 m, and can even reach 300 m, when the current is changed between 50 mA and +50 mA.

So, we can simply regulate the movement of the lenses to the required position by keeping the VCM displacement at the linear region. For better performance of upward and downward displacement, the hysteresis tolerance and gravity of the lens system have been considered in our design.

The VCM4 z-value was tuned to make the concentrated spot size comparable to the fiber core size in order to provide optimal coupling efficiency. A collimated laser beam of wavelength and diameter DB needs to be coupled onto a fiber with a mode field diameter dF, according to Gaussian optics. , the coupling lens focal length should be

$f = \pi DB\ dF\ /4\lambda$.

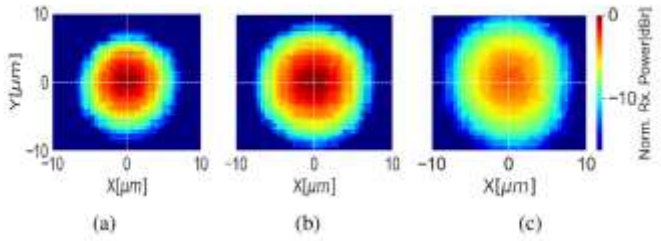

Fig. H. Received optical power profile for different z value of VCM4. (a) z = 0. (b) z = −90 μm. (c) z = −175 μm.

The received optical power profile for VCM 4, which is employed for fiber coupling, is plotted in Fig. H. The power values were obtained using a 10 mm SMF core, by spiraling the x and y axes of the VCM4 lens, and for three different z positions (0, 90, and 175 mm). We can simply control the fiber coupling efficiency for better system performance because of the VCM linearity. In fact, the power profile at the fiber core exhibits Gaussian behavior for the incident collimated beam.

Hence, the power profile size and peak power can be effectively regulated by altering the z value.

3. Design Principle and Method of MABBMs

Butler matrix (WANG Y et al., 2018), (DYAB et al., 2018) is a type of passive multiport network that features many phase differences, low loss, a low profile, and a simple structure. It has found widespread use as an aerial feeding network for multi-beam radiation. When an antenna array of M elements is coupled to a N M Butler matrix, the input ports can be simultaneously energized to produce N independent beams pointing in various directions. Here is a detailed explanation of the Butler matrix-based multi-beam antennas' operating principles and design methodology.

3.1 Principles of Operation for MABBMs

An antenna array's mechanism for producing multi-beam radiation is examined using the beam-scanning theory of the antenna array, and the results can be utilized to inform the thorough design of MABBMs. The beam-scanning angle 0 of a linear antenna array can be determined using the comprehensive theory of antenna arrays. (BALANIS, 1996)

$$\theta 0 = \arcsin (- \varphi \lambda 2\pi d),$$

(1) where φ and d explain the phase difference and gap between related neighboring items, and λ illustrates, using the schematic design in Fig. 2, the wavelength connected to the operating frequency in vacuum.

(2) It can be seen from Eq. (1) that the wavelength, which corresponds to the antenna's operating frequency, the phase difference, and the distance d between neighboring elements all affect the antenna array's beam-scanning direction.

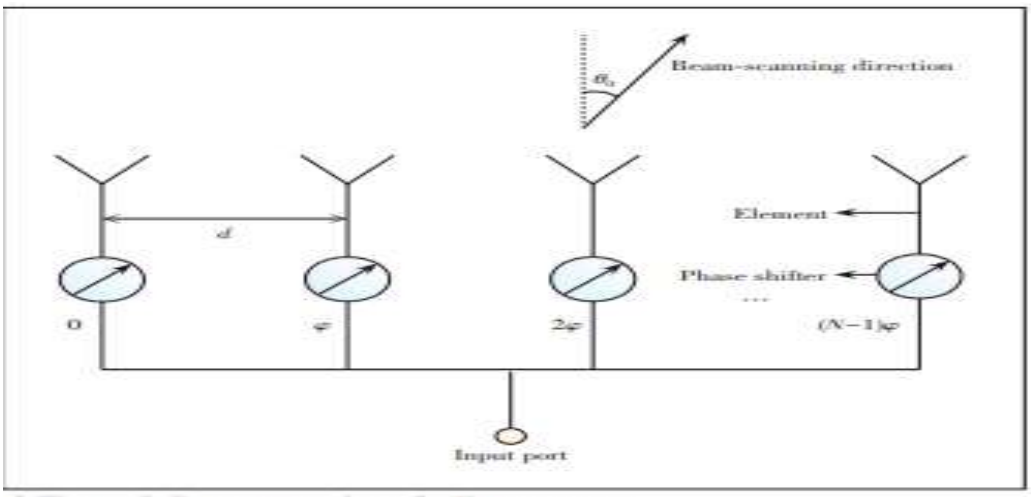

▲ Figure 2. Beam-scanning of a linear array.

The beam scanning direction of the array is simply governed by the phase difference of neighboring elements after the working frequency and spacing have been chosen, and various phase differences result in various beam-scanning orientations. An antenna array can radiate numerous beams in various directions when several signals with various phase differences simultaneously excite it, a process known as multi-beam emission. The radiation pattern of a three-beam antenna array powered by a 3 5 Butler matrix at 2.2 GHz is depicted in Fig. 3.

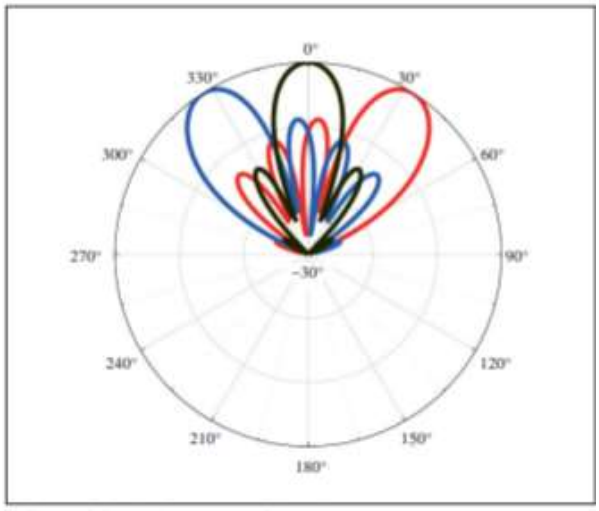

▲Figure 3. Radiation pattern of three-beam antenna array.

A half-wavelength electric dipole makes up the element, and there is a 75 mm gap between each one. The excitation of the array has 120o, 0o, and +120o identical amplitude and phase differences. It is evident that the MABBM has been able to successfully produce 3 beams that point in three separate directions.

3.2 Design Method of MABBMs

Two varieties of the MABBMs' multi-beam radiation are used in practical applications: 2D multiple beams in both the horizontal and vertical planes (LIAN et al., 2018), (KIM et al., 2016) and multiple beams in either the horizontal plane or the vertical plane (TAJIK et al., 2019), (SHAO Q et al., 2019). This study presents the design technique of MABBMs with numerous beams in the horizontal plane, which simplifies the analysis without losing generality. Similar design principles can be used to create additional types of 2D MABBMs. According to Figs. 4a, 4b, and 4c, respectively, a 1D MABBM is typically composed of a M L array, N M Butler matrices, and L-way power dividers.

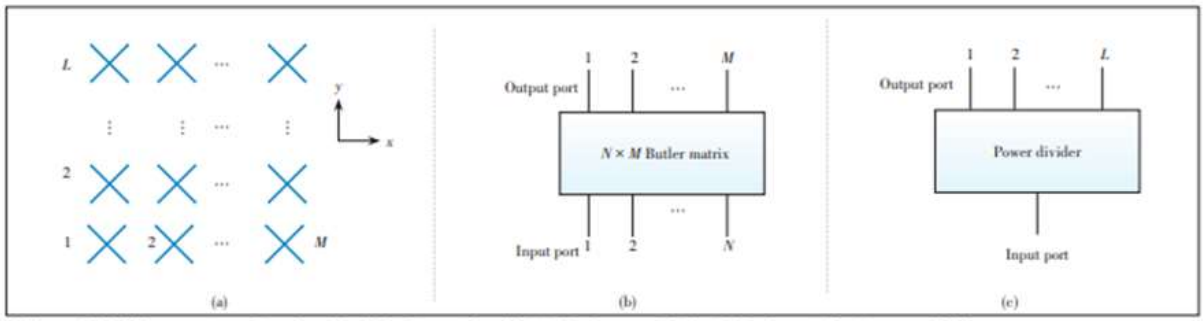

▲Figure 4. Multi-beam antenna based on $N \times M$ Butler matrix with (a) $M \times L$ array; (b) $N \times M$ Butler matrix; (c) power divider.

The design steps of the MABBM can be summarized as follows.

Executing the N–M Butler matrix is the first step. First, the number (N) of an MABBM's radiation beams and Butler matrix's input ports are established.

The number of radiation beams and the communication capacity are correlated, with more radiation beams offering more capacity.

By multiplying the necessary communication capacity by the Butler matrix's number of input ports, one may get the number of radiation beams. The Butler matrix's output port numbers (M), as well as its amplitude and phase difference, are then determined by the side lobe level needed for each beam. Based on the aforementioned rationale, the N M Butler matrix is created to satisfy the bandwidth, amplitude, and phase difference specifications.

Creating a M–L array is step two. The Butler matrix's output port count (M) determines the number of elements in the array's horizontal plane, and the needed gain (L) determines the number of elements in the array's vertical plane. Also, the cross level between adjacent beams and the spacing between adjacent parts in the horizontal plane both have a significant impact on the coverage area of the multiple beams and should be carefully chosen. On this foundation, the antenna element is created to fulfill the demands of the requisite bandwidth, and the necessary M L array is then put into practice.

Step 3: Implementing the MABBM. For the purpose of implementing the suggested multi-beam antenna, each power splitter's input port is first linked to the output port of the Butler matrix using 50 coaxial cables, followed by the output port of the antenna element in the vertical plane. 4 Recent MABBMs for Base-Station Applications Research Progress Several MABBMs have been proposed recently for use in mobile communication applications.

A small dual band two-beam 4* 8 antenna array with dual polarizations is suggested (ZHANG et al., 2017) for base station applications.

Two 4* 4 sub arrays operating in the 3G (1 710-2 170 MHz) and long-term evolution (LTE) (2 490-2 690 MHz) bands make up this system.

The elements of the two 4* 4 sub arrays are interconnected for size downsizing, as depicted in Fig. 5a.

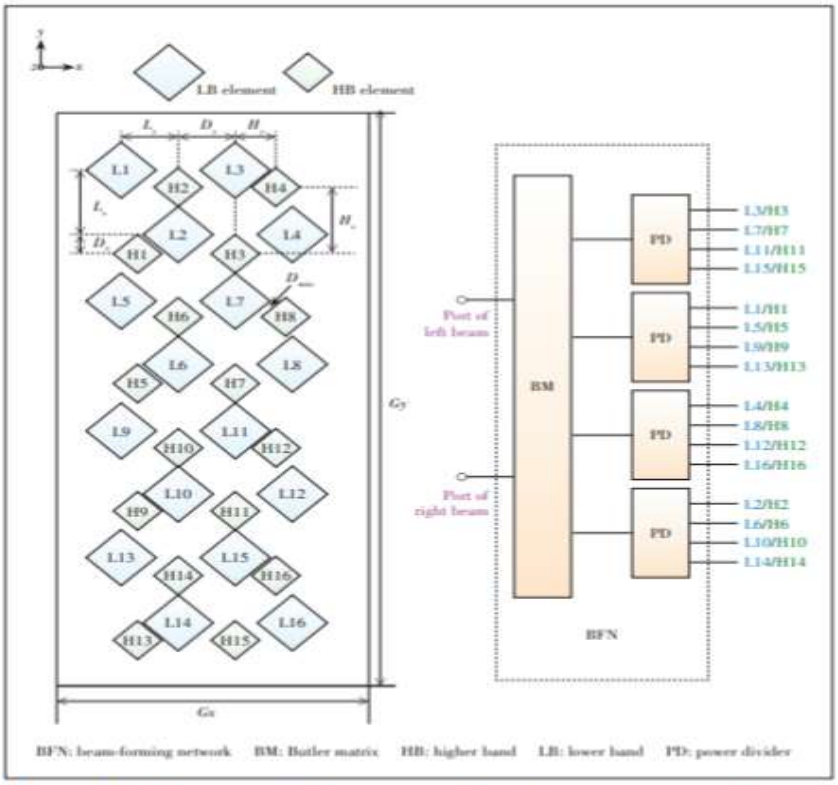

▲ **Figure 5. Dual-band two-beam antenna in Ref. [34]. (a) Elements distribution of the interleaved configuration; (b) Beam forming network diagram.**

By utilizing filtering antennas (DUAN et al., 2016) with out-of-band radiation suppression, the mutual coupling between the elements operating at different bands is suppressed. Beam-forming networks with minimal magnitude and phase imbalances are specifically created for each band in order to provide stable two-beam radiation patterns within the two operating bands.

Fig. 5b presents the beam-forming network's configuration. Four filtering power dividers and a 2 x 4 Butler matrix make up the structure (PDs). The two full bands of the array show a consistent 10 dB beam width approximately 120° in the azimuth plane, and the two beam radiation patterns meet the base station applications' need for coverage of 120° in the azimuth plane.

Moreover, within the two operational bands, 16.4 dBi/15.5 db peak gains and roughly 10 db cross levels at the intersection of two beams are attained.

A wideband dual-polarized 4 6 antenna array with two beams is offered (YE L H et al., 2019) for base station applications. The arrangement of its three 4 2 sub arrays is depicted in Fig. 6a. A wide band crossed dipole is used as the fundamental component to produce 45° dual polarized radiation. The lower and top 4 1 sub arrays for each 4 *2 sub array are out of alignment in the horizontal plane.

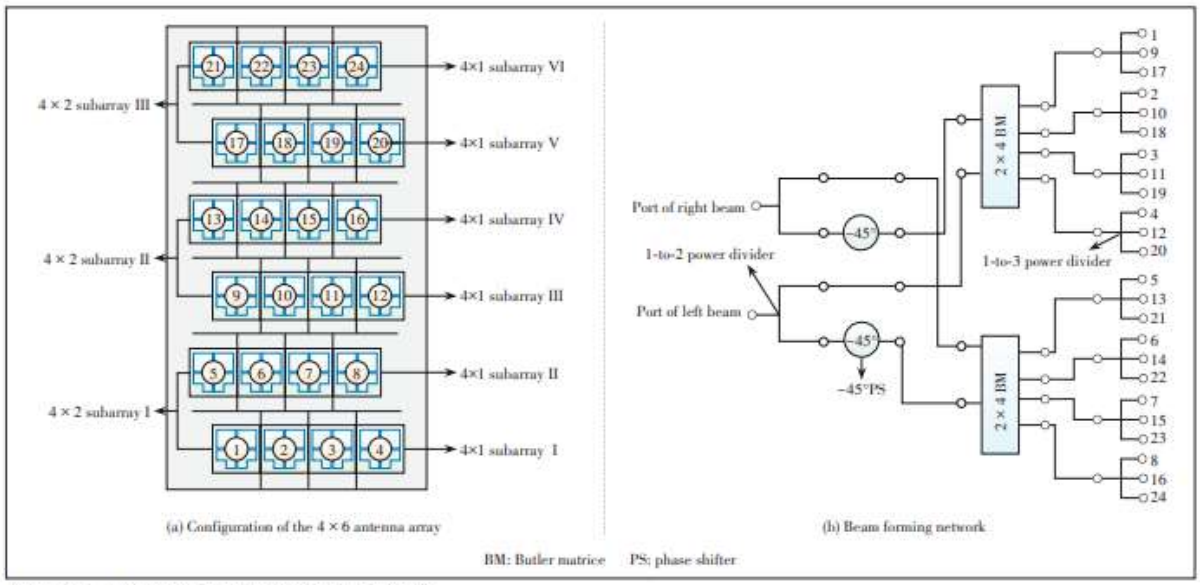

▲Figure 6. Wideband two-beam antenna in Ref. [36].

This results in good grating-lobe suppression since the 4 *2 sub array is similar to an 8* 1 sub array with half of the neighboring element spacing.

Certain wideband beam-forming net works with minor magnitude and phase imbalances are developed to achieve stable two-beam radiation with little side lobe over a wide frequency spectrum. Figure 6b displays the beam-forming network diagram. It is made up of eight 1-to-3 power dividers, two 1-to-2 power dividers, two phase shifters (PSs) at 45 degrees, two Butler matrices (BMs), and two 1-to-2 power dividers.

Moreover, the neighboring element spacing is improved to achieve a consistent 10 dB beam width around 120°, satisfying the base station application's need for coverage of 120° in the horizontal plane.

In the horizontal plane, the array's two beams have a constant 10 dB beam width of about 120 degrees and a cross level of roughly 10 dB. For voltage standing wave ratio, the impedance bandwidth is determined to be 56.1% (1.64 - 2.92 GHz) (VSWR)

Butler matrices-based broad band three-beam antenna arrays are reported (ZHU et al., 2019) and used to boost the capacity of 3G/LTE base stations. A wideband 3 3 Butler matrix, made up of fixed wideband phase shifters and quadrature couplers, is the key component of three-beam arrays. Strip lines are used to implement phase shifters and wideband quadrature. 1.7–2.7 GHz.

Beam-forming networks made up of augmented 3 3 Butler matrices and power dividers are suggested in order to increase the number of output ports from three to five or six, as shown in Figs. 7a and 7b, respectively, in order to achieve the appropriate beam width and the necessary crossed level between adjacent beams. With strong impedance matching, high beam isolation, and three-beam radiation in the horizontal plane over the broad frequency range of 1.7-2.7 GHz, dual-polarized, three-beam antenna arrays with five and six elements are created to span the 3G/LTE spectrum.

A dual-layer 4* 8 Butler matrix-fed compact four-beam slot antenna array with side lobe level suppression provided by substrate integrated waveguide technology is proposed. (LIAN et al., 2018)

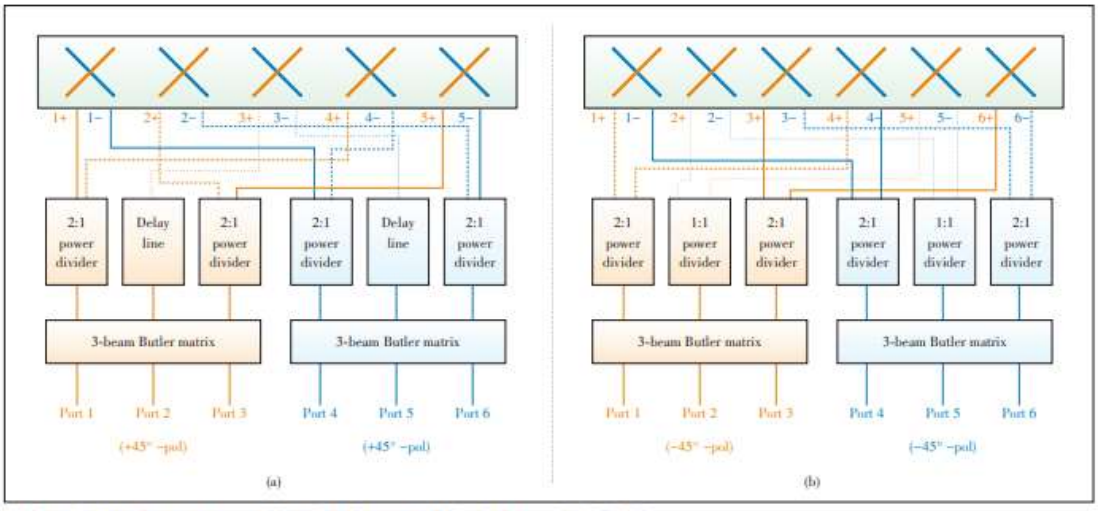

▲Figure 7. Three-beam antennas with (a) five elements and (b) six elements in Ref. [37].

A novel dual-layer structure made up of a 4 4 Butler matrix and an amplitude ta per is suggested to alleviate the issue of the excessive crossovers in the traditional 4 8 Butler matrix,

As shown in Fig. 8a. In order to reduce side lobe level, the amplitude taper is used to transform the four outputs with equal power divisions into eight outputs with unequal power distributions from the four outputs with equal power divisions provided by the 4 4 Butler matrix.

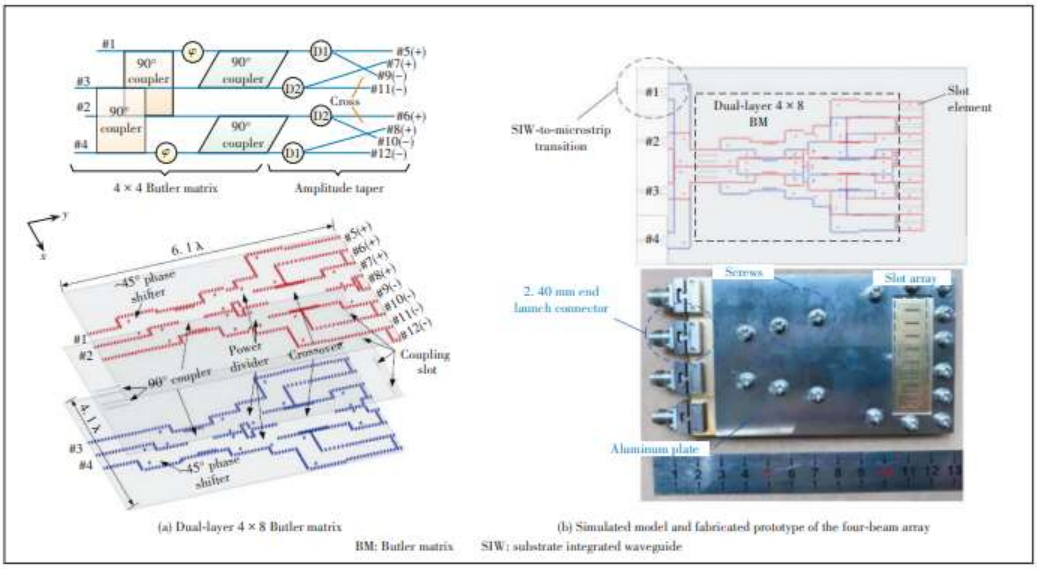

▲Figure 8. Four-beam array in Ref. [38].

To reduce the number of needed crossovers from the original five sets to just one set, the proposed topology of the 4* 8 Butler matrix is used. To attain improved compactness, the 4* 8 Butler matrix can therefore be greatly simplified. In order to produce four-beam radiation with low side lobe level, an eight-element slot antenna array is fed by the suggested BM. The simulated model and prototype are illustrated in Fig. 8b.

By adding two sets of vertical linkages to the standard array layout, a modified topology of a 2D multi beam antenna array (LI Y J et al., 2017) supplied by a passive beam forming network is proposed to significantly boost the communication capacity.

In contrast to the conventional design, the proposed array structure in Fig. 9 may be easily incorporated onto multi-layered planar substrates, which has advantages for millimeter wave applications such as low loss characteristics, ease of realization, and low fabrication cost. The next step is to create a 4 4 multi beam aerial array that can produce 16 beams.

Future millimeter wave wireless systems utilized for 5G/B5G communications might find it advantageous to create the relatively large size 2D multi beam antenna arrays with planar passive beam forming networks using the proposed array topology.

5. Challenges of MABBMs

As mobile communication technology advances quickly, mobile communication systems move in the direction of various frequency bands, miniaturization, and low cost, which results in the following

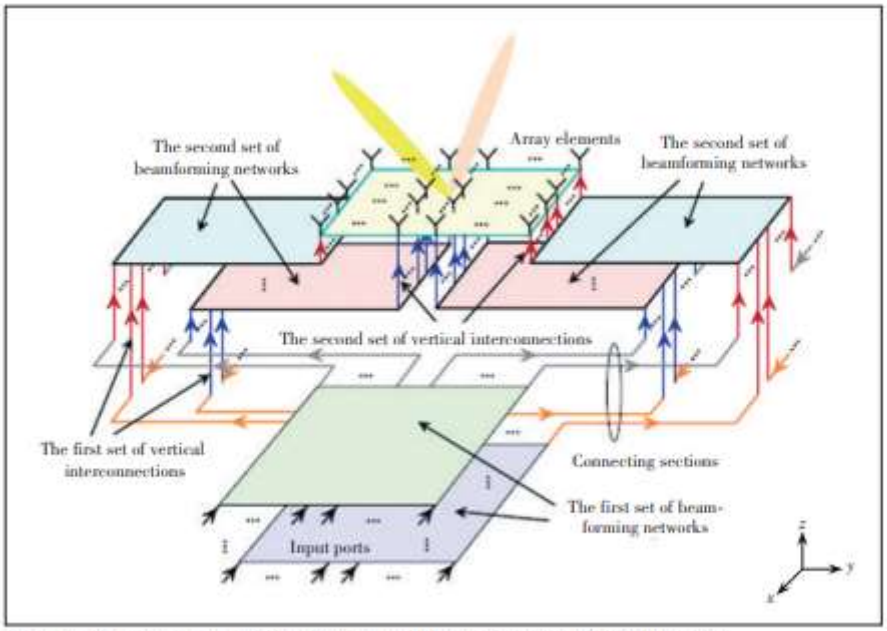

Figure 9. Configuration of the planar 2D multibeam antenna array in Ref. [39].

5.1. Challenges for MABBMs.

(1) Wideband or multi-band MABBM design Mobile communication technologies including 2G, 3G, 4G, 5G, and B5G will coexist for a very long time in the future in the 5G/B5G era. An MABBM must cover numerous communication frequency bands in order to adhere to the development trend of mobile communication, reduce the number of antennas, and increase the usage of space resources and spectrum resources. Thus, it is extremely difficult to create a broadband or multi-band MABBM with strong impedance matching, high beam isolation, and effective side lobe suppression..

(2) MABBM miniaturization Mobile communication system spacing and cost can both be decreased with the use of miniature MABBMs. The Butler matrix must be smaller, and the space between antenna elements must be closer, in order to miniaturize MABBMs.

Strong electromagnetic coupling and radiation interference would be introduced as a result, leading to issues like deteriorated beam solation and distorted radiation pattern.

Hence, another difficulty is miniaturizing an MABBM with good electrical and radiation performance.

6. Conclusions

In summary, this research has reviewed the MABBM technologies. The requirements for base station applications, the operating principles, the design, and the implementation of MABBMs are discussed, and the most recent advancements in research on broadband or multi-band MABBMs are reviewed. The entire MABBM is viewed as a possible path towards the development of high-performance 3G/LTE/5G/B5G mobile communication systems, even though a few related challenges need to be resolved.

7. References

LI M, LI Q L, WANG B, et al. (2018). A low-profile dual-polarized dipole antenna using wideband AMC reflector [J]. IEEE transactions on antennas and propagation, 66(5): 2610–2615. DOI:10.1109/tap.2018.2806424

WANG J, WANG W, LIU A M, et al. (2020). Cross-polarization suppression of a dual-polarized microstrip antenna using enclosed substrate - integrated cavities [J]. IEEE antennas and wireless propagation letters, 19(1): 64 – 68. DOI: 10.1109/lawp.2019.2953076

WANG X Y, TANG S C, YANG L L, et al. (2020). Differential -fed dual -polarized di- electric patch antenna with gain enhancement based on higher order modes [J]. IEEE antennas and wireless propagation letters, 19(3): 502–506. DOI: 10.1109/lawp.2020.2964569

SAEIDI-MANESH H, SAEEDI S, ZHANG G F. (2020). Dual-polarized perpendicularly fed balanced feed antenna with high polarization purity [J]. IEEE antennas and wireless propagation letters, 19(2): 368 – 372. DOI: 10.1109/ lawp.2020.2963958

HUANG H, LI X P, LIU Y M. (2020). A low -profile, single -ended and dual -polarized patch antenna for 5G application [J]. IEEE transactions on antennas and propa- gation, 68(5): 4048–4053. DOI:10.1109/tap.2019.2948743

SUDHAKAR RAO K, MORIN G A, TANG M Q, et al. (1995). Development of a 45 GHz multiple - beam antenna for military satellite communications [J]. IEEE transac- tions on antennas and propagation, 43(10): 1036 – 1047. DOI: 10.1109/ 8.467639

EGAMI S. (1999). A power-sharing multiple-beam mobile satellite in Ka band [J]. IEEE journal on selected areas in communications, 17(2): 145 – 152. DOI: 10.1109/49.748778

RAHMAT-SAMII Y, DENSMORE A C. (2015). Technology trends and challenges of an- tennas for satellite communication systems [J]. IEEE transactions on antennas and propagation, 63(4): 1191–1204. DOI:10.1109/tap.2014.2366784

ZHANG Z Y, ZHAO Y R, LIU N W, et al. (2019). Design of a dual-beam dual-polarized offset parabolic reflector antenna [J]. IEEE transactions on antennas and propa- gation, 67(2): 712–718. DOI:10.1109/tap.2018.2882593.

CHOU H T, CHOU S J, CHIU C W, et al. (2018). Quasi-orthogonal multibeam radia- tion of reflector antennas for radio coverage of mobile communication at milli- meter - wave frequencies [J]. IEEE transactions on antennas and propagation, 66(11): 6340–6345. DOI:10.1109/tap.2018.2861988

MANOOCHEHRI O, DARVAZEHBAN A, SALARI M A, et al. (2018). A parallel plate ultra wideband multibeam microwave lens antenna [J]. IEEE transactions on antennas and propagation, 66(9): 4878 – 4883. DOI: 10.1109/ tap.2018.2845548

LIAN J W, BAN Y L, CHEN Z, et al. (2018). SIW Folded Cassegrain lens for millimeter wave multibeam application [J]. IEEE antennas and wireless propagation letters, 17(4): 583–586. DOI:10.1109/lawp.2018.2804923

LARIMORE Z, JENSEN S, GOOD A, et al. (2018). Additive manufacturing of lune- burg lens antennas using space - filling curves and fused filament fabrication [J]. IEEE transactions on antennas and propagation, 66(6): 2818–2827. DOI:10.1109/tap.2018.2823819

MEI Z L, BAI J, NIU T M, et al. (2012). A half maxwell fish-eye lens antenna based on gradient-index meta materials [J]. IEEE transactions on antennas and propagation, 60(1): 398–401. DOI:10.1109/tap.2011.2167914

HUANG M, YANG S W, GAO F, et al. (2014). A 2-D multibeam half maxwell fish-eye lens antenna using high impedance surfaces [J]. IEEE antennas and wireless propagation letters, 13: 365–368. DOI:10.1109/lawp.2014.2306207

KWON D H, WERNER D H. (2009). Beam scanning using flat transformation electro-magnetic focusing lenses [J]. IEEE antennas and wireless propagation letters, 8: 1115–1118. DOI:10.1109/lawp.2009.2033619

JIANG Z H, GREGORY M D, WERNER D H. (2012). Broadband high directivity mul-tibeam emission through transformation optics - enabled metamaterial lenses [J]. IEEE transactions on antennas and propagation, 60(11): 5063 – 5074. DOI:10.1109/tap.2012.2207685

WU Q, HIROKAWA J, YIN J X, et al. (2018). Millimeter-wave multibeam end fire du- al - circularly polarized antenna array for 5g wireless applications [J]. IEEE transactions on antennas and propagation, 66(9): 4930 – 4935. DOI: 10.1109/tap.2018.2851667

LI Y J, WANG J H, LUK K M. (2017). Millimeter -wave multibeam aperture -coupled magnetoelectric dipole array with planar substrate integrated beamforming net- work for 5G applications [J]. IEEE transactions on antennas and propagation, 65(12): 6422–6431. DOI:10.1109/tap.2017.2681429

KIM D H, HIROKAWA J, ANDO M. (2016). Design of waveguide short-slot two-plane couplers for one-body 2-D beam-switching butler matrix application [J]. IEEE transactions on microwave theory and techniques, 1–9. DOI:10.1109/ tmtt.2016.2515605

ZHONG L H, BAN Y L, LIAN J W, et al. (2017). Miniaturized SIW multibeam anten- na array fed by dual-layer 8 × 8 Butler matrix [J]. IEEE antennas and wireless propagation letters, 16: 3018–3021. DOI:10.1109/lawp.2017.2758373

LIAO W J, TUAN S K, LEE Y, et al. (2018). A Diversity receiver - based high - gain broad-beam reception array antenna [J]. IEEE antennas and wireless propaga- tion letters, 17(3): 410–413. DOI:10.1109/lawp.2018.2792438

WINCZA K, STASZEK K, GRUSZCZYNSKI S. (2017). Broadband multibeam antenna arrays fed by frequency - dependent butler matrices [J]. IEEE transactions on antennas and propagation, 65(9): 4539 – 4547. DOI: 10.1109/ tap.2017.2722823

HONG W, JIANG Z H, YU C, et al. (2017). Multibeam antenna technologies for 5G wireless communications [J]. IEEE transactions on antennas and propagation, 65(12): 6231–6249. DOI:10.1109/tap.2017.2712819

WANG Y Q, MA K X, JIAN Z. (2018). A low -loss Butler matrix using patch element and honeycomb concept on SISL platform [J]. IEEE transactions on microwave theory and techniques, 66(8): 3622 – 3631. DOI: 10.1109/tm- tt.2018.2845868

DING K J, KISHK A A. (2018). 2D Butler matrix and phase - shifter group [J]. IEEE transactions on microwave theory and techniques, 66(12): 5554–5562. DOI:10.1109/tmtt.2018.2879013

DYAB W M, SAKR A A, WU K. (2018). Dually -polarized Butler matrix for base sta- tions with polarization diversity [J]. IEEE transactions on microwave theory and techniques, 66(12): 5543–5553. DOI:10.1109/tmtt.2018.2880786

BALANIS C A. (1996). Antenna theory: analysis and design [M]. Hoboken, USA: Wiley.

TAJIK A, SHAFIEI ALAVIJEH A, FAKHARZADEH M. (2019). Asymmetrical 4 × 4 Butler matrix and its application for single layer 8 × 8 Butler matrix [J]. IEEE transactions on antennas and propagation, 67(8): 5372 – 5379. DOI: 10.1109/tap.2019.2916695

SHAO Q, CHEN F C, WANG Y, et al. (2019). Design of modified 4 × 6 filtering butler matrix based on all - resonator structures [J]. IEEE transactions on microwave theory and techniques, 67(9): 3617 – 3627. DOI: 10.1109/tm- tt.2019.2925113

LIAN J W, BAN Y L, YANG Q L, et al. (2018). Planar millimeter-wave 2D beam-scan- ning multibeam array antenna fed by compact SIW beam-forming network [J]. IEEE

transactions on antennas and propagation, 66(3): 1299 – 1310. DOI:10.1109/tap.2018.2797873

LI Y J, LUK K M. (2016). 60-GHz dual-polarized two-dimensional switch-beam wide- band antenna array of aperture - coupled magneto - electric dipoles [J]. IEEE transactions on antennas and propagation, 64(2): 554 – 563. DOI: 10.1109/tap.2015.2507170

ZHANG X Y, XUE D, YE L H, et al. (2017). Compact dual-band dual-polarized inter- leaved two-beam array with stable radiation pattern based on filtering elements [J]. IEEE transactions on antennas and propagation, 65(9): 4566–4575. DOI:10.1109/tap.2017.2723914

DUAN W, ZHANG X Y, PAN Y M, et al. (2016). Dual-polarized filtering antenna with high selectivity and low cross polarization [J]. IEEE transactions on antennas and propagation, 64(10): 4188–4196. DOI:10.1109/tap.2016.2594818

YE L H, ZHANG X Y, GAO Y, et al. (2019). Wideband dual-polarized two-beam an- tenna array with low sidelobe and grating-lobe levels for base-station applica- tions [J]. IEEE transactions on antennas and propagation, 67(8): 5334– 5343. DOI:10.1109/tap.2019.2913795

ZHU H, SUN H H, JONES B, et al. (2019). Wideband dual-polarized multiple beam- forming antenna arrays [J]. IEEE transactions on antennas and propagation, 67(3): 1590–1604. DOI:10.1109/tap.2018.2888728

LIAN J W, BAN Y L, XIAO C H, et al. (2018). Compact substrate -integrated 4 × 8 Butler matrix with sidelobe suppression for millimeter -wave multibeam appli- cation [J]. IEEE antennas and wireless propagation letters, 17(5): 928– 932. DOI:10.1109/lawp.2018.2825367

I. A. Ivan, M. Ardeleanu, and G. J. Laurent, (2012). “High dynamics and precision optical measurement using a position sensitive detector (PSD) in reflection-mode: Application to 2D object tracking over a smart surface,” Sensors, vol. 12, no. 12, pp. 16771–16784.

Abdel moula Bekkal. (2022). New Generation Free-Space Optical Communication Systems With Advanced Optical Beam Stabilizer, JOURNAL OF LIGHTWAVE TECHNOLOGY, VOL. 40, NO. 5, MARCH 1.

Doi: doi.org/10.52132/Ajrsp.en.2023.48.2